60 GHz Optimised Nickel-free Gold-plated Enclosed Coplanar Waveguide Liquid Crystal Phase Shifter

Jinfeng Li*[1,2]
*[1]*Centre for Electronics Frontiers, University of Southampton,* Southampton, SO17 1BJ, United Kingdom
[2]*Department of Electrical and Electronic Engineering, Imperial College London,* London, SW7 2AZ, United Kingdom
*Jinfeng.Li@soton.ac.uk

***Abstract*—A novel nickel-free gold-plated enclosed coplanar waveguide is experimentally demonstrated for a liquid crystal tunable delay line phase shifter at 60 GHz. By numerical investigations, we find that conventional surface impedance model (without meshing inside metals) fails to accurately characterise the effect of gold-plating thickness on conductor loss, especially when the plating thickness is smaller than 4 times of the gold's skin depth. To address this, adaptive meshing inside metals is performed for accurate modelling of the device. The gold-plating thickness is then experimentally optimised and tailored for the liquid crystal-based device-making procedures, i.e. taking into account the accelerated copper migration into gold problem during the alignment agent baking process at 200˚C. Measurement results of assembled phase shifters at 60 GHz verify that a direct gold plating of 2µm on Cu can reduce the insertion loss by 1.79 dB and 2.85 dB as compared with that with a thinner plating of 50 nm, and no plating, respectively. The maximum insertion loss of -2.996 dB demonstrated at 60 GHz for the 0-π phase shifter delivers a figure-of-merit of 60˚/dB, an improvement of 42˚/dB as compared with up-to-date literature.**

Keywords—enclosed coplanar waveguide, gold plating, insertion loss, liquid crystal, millimetre wave, phased array, tunable delay line

I. INTRODUCTION

Millimetre-wave phased array antenna beam steering has been playing a big part in the ongoing 5G wireless communication networks rollout for indoor short-range communications, such as supplying wireless multimedia in airplane or car cabins [1]. Phase shifters, as the key feeding components underpinning the phased array technology, have attracted tremendous research and development interest [2], targeting a low insertion loss and a high resolution of phase shift. Among state-of-the-art technologies in realising this, tunable delay line method based on highly anisotropic liquid crystal (LC) as tunable dielectrics has pushed the limit of planar microwave transmission line implementation from 10 GHz microstrip [3][4] to 60 GHz enclosed coplanar waveguide (ECPW) [5], and progressively towards 90 GHz high-aspect-ratio coplanar waveguide [6] that challenges the current status of manufacturing in terms of electrodes patterning and LC alignment.

With the decrease of wavelength from microwave to millimetre-wave, device's performance degradation less observable at the microwave bands can, however, be noticeable in the millimetre-wave frequencies. To our knowledge, high insertion loss at millimetre wave remains the key challenge of LC-based planar phase shifter solution when competing with those realised in low-loss waveguides.

Given a LC-based phase shifter is impedance matched with negligible return loss, decomposing insertion losses dissipated in different materials (i.e. conductors and dielectrics) is highly desirable for device optimisation. However, it is technically infeasible to experimentally separate conductor loss and dielectric loss from a measured S_{21} with a vector network analyser. To partially address this, numerical simulations based on theoretical analysis model of conductor and dielectric losses [6] are carried out to inform decisions on device optimisations. With this approach, total insertion loss mitigation is demonstrated in our LC-based ECPW phase shifters for 54-66 GHz applications [5]. However, for a practical performance-measurement of a fabricated LC-based device, higher-than-expected metal loss can occur because of accelerated copper oxidation (during the alignment agent baking process at 200˚C for 20 minutes) not considered at the design stage, hence the need for surface finish (e.g. gold plating in this study). While traditional electroless nickel immersion gold (ENIG) based surface-plating method is highly lossy due to the resistive nickel barrier, this work reports a novel nickel-free gold plating of an optimum thickness directly on copper for a low-loss ECPW LC-based phase shifter at 60 GHz shown in Fig. 1.

Section II of the paper numerically simulates the effect of gold-plated thickness on insertion loss, with two modelling methods compared, i.e. meshing inside metals versus tradition surface impedance model without meshing inside metals. Section III presents the fabricated substrates with different thicknesses of gold plated. Measured insertion losses of assembled phase shifter devices are compared for validation of the optimum gold plating thickness.

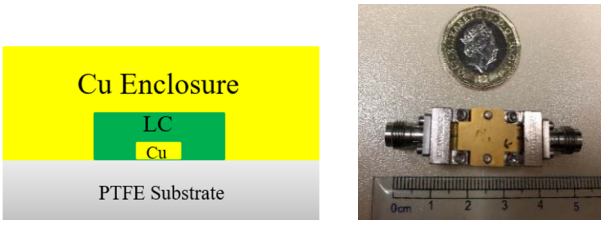

(a) (b)

Fig. 1. ECPW LC phase shifter (a) structure; (b) photo of fabricated device.

II. Simulation of Gold-plated ECPW LC Phase Shifter

A. Surface Impedance Model vs. Meshing inside Metals

The penetration depth (δ) at 60 GHz is 0.31μm for gold (Au), and 0.26μm for copper (Cu). Modern computational electromagnetics software packages (e.g. HFSS and CST) take the representation of conductors by default as surface impedance Z_s following Eq. (1):

$$Z_s = \frac{e^{kt} + \frac{\sigma z_c - k}{\sigma z_c + k} e^{-kt}}{e^{kt} - \frac{\sigma z_c - k}{\sigma z_c + k} e^{-kt}} \times \frac{k}{\sigma} \quad (1)$$

where $k=(1+j)/\delta$, and $z_c = \sqrt{\mu_0/\varepsilon_0}$ represents characteristic impedance of free space. This treatment only performs meshing and computing the fields at the conductor surface and in the space outside the conductors, while the space inside conductors is not meshed. The effects of the internal fields are considered by a surface impedance model, given that the internal fields fall exponentially with the distance from the surface.

We perform 60 GHz simulations for the LC-based ECPW (Fig. 1) with 0.5oz Cu clad (thickness T_{Cu} =17μm=65 δ_{Cu}) laminated on a PTFE substrate, with gold plating not considered first. Comparative study on insertion loss calculation is conducted based on two models. Model 1 is based on HFSS's default surface impedance model without meshing inside metals. Model 2 is adaptive meshing inside metals, solving the internal field of the metals, refining volume and surface meshes where the field gradients are high. Convergence of the adaptive-meshing refinement inside the core line metal is shown in Fig. 2. Benchmarking the two methods, it is numerically verified that S_{21} given by the surface impedance model (no meshing inside metals) agrees with that by meshing inside conductors. However, it is not the case for a thin layer of gold plating on the Cu patterns. For the same LC-based ECPW geometry, we simulate gold-plated Cu with gold thickness T_{Au} varying from 0 to 4μm (i.e. from 0 to 16 times of δ_{Au} at 60GHz). Fig. 3 presents S_{21} versus the ratio of gold-plating thickness to gold's skin depth (T_{Au}/δ_{Au}) at 60 GHz. It is clearly observed that traditional surface impedance model fails to accurately model the gold plating cases with $T_{Au} < 4\delta_{Au}$. Instead, it over-estimates the conductor loss by up to 0.3 dB/cm. S_{21} levels off when $T_{Au} > 4\delta_{Au}$, beyond which both models agree in statistics.

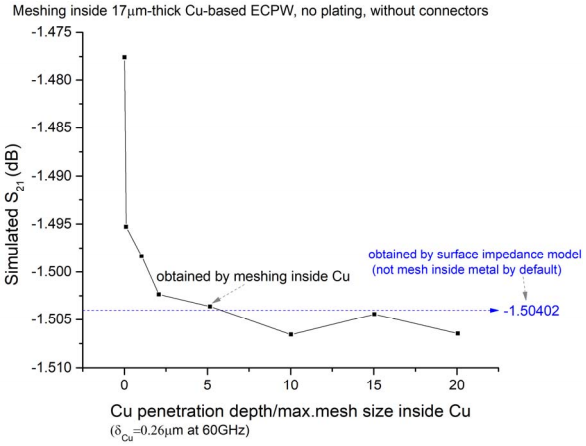

Fig. 2. Agreements between two modelling methods when $T_{Cu} >> \delta_{Cu}$.

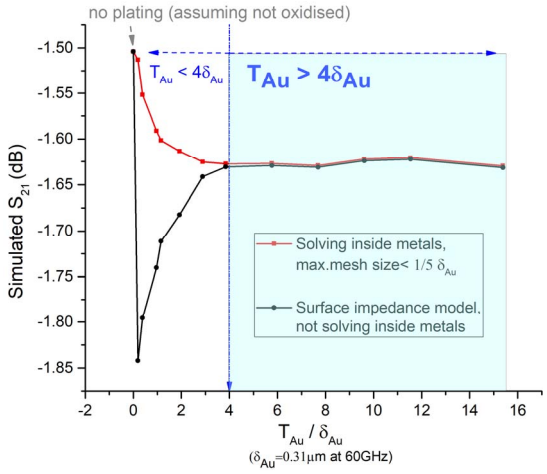

Fig. 3. Simulated impact of gold-plating thickness on insertion loss (60GHz).

In a summary, for conductor thickness well above the penetration depth, surface impedance model (not solving inside metals) works fine with the advantage of reduced computation burden. However, for structures in which penetration depth of the field is of the same order as the plated conductor thickness (e.g. for $T_{Au} < 4\delta_{Au}$ in this work), substantial errors can occur in the loss estimation. In this situation, meshing and solving inside the plated metal can accurately represent the field's decaying behaviour without overestimation of the conductor loss.

B. Limitation due to Cu Migration into Gold and Oxidation

From Fig. 3, the addition of gold finish degrades S_{21} due to increased resistance as compared with non-plated pure Cu (assuming oxidisation not happened). However, at elevated temperature when baking the LC's alignment solvent, an inadequate thickness of pure gold deposited on PCB can result in a diffusion of Cu atoms into gold (tarnishing), exposing the copper and ultimately a formation of oxide layer which degrades the electrical conductivity, as demonstrated by the experiment results shown later in Figs. 5 and 6. Out of this concern, the plated gold should be thick enough compared with the Cu foil underneath. Note that etching and plating errors both increase dramatically with the plating thickness, resulting in a substantial deviation from the ideal right-angle design of the conductor profile. Optimisation of the gold-plated thickness in this study is arguably a compromise upon the theoretical insertion loss derivation and the practical limitations from the LC-based device manufacturing procedures.

III. Device Fabrication and Measurement Results

Photolithographically patterned Cu-based substrates are surface-finished with gold following a nickel-free electrolytic process. Thickness of the gold plating is experimentally investigated for a reliable protection without degrading the conductor's performance especially after the 200˚C baking (for evaporating solvent of the coated alignment agent on substrate [7]). Different thicknesses of gold plating from 0 (non-plated) to 3μm are performed for an array of CPW substrates with 0.5oz Cu foil. Fig. 4 shows the gold-plated substrates at room temperature. After 200˚C baking for 20 minutes, the same groups of substrates are inspected again, with their profiles illustrated in Fig. 5.

(a) (b) (c)

Fig. 4. 27˚C profile: (a) non-plated; (b) 50nm plated; (c) 2µm plated.

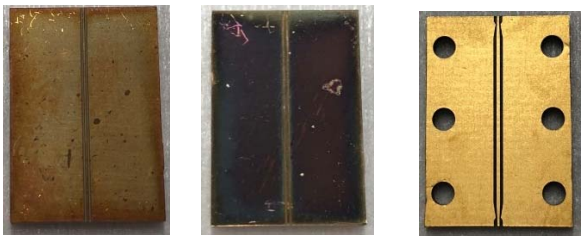

(a) (b) (c)

Fig. 5. Post-baked profile: (a) non-plated; (b) 50nm plated; (c) 2µm plated.

Comparing Fig. 5 (b) with Fig. 4 (b) for the 50nm gold-plated substrate, tarnishing occurs after the 200˚C heating as Cu atoms migrate into gold (an irreversible process), which raises a problem of Cu oxide layer formation and dramatically increases the resistance, as evidenced by the insertion loss measurement in Fig. 6 for the assembled phase shifters with different gold plating thicknesses but with a same delay line length for π shift at 60 GHz. For device with non-plated Cu conductors (oxidised), measured maximum deterioration of insertion loss is up to 4.5 dB at 64 GHz when compared with device plated with 2µm. This indicates that relying purely on polyimide coating (alignment agent) has a limited scope in preventing oxidation of the bare Cu. The insertion loss degradation is even worse for the 50nm gold-plated device above 65 GHz, as the coexistence of the tarnishing and oxidising effects exacerbates the increase of metal loss by 3.4 dB at 67 GHz as compared with the non-plated device (oxidised but not tarnished).

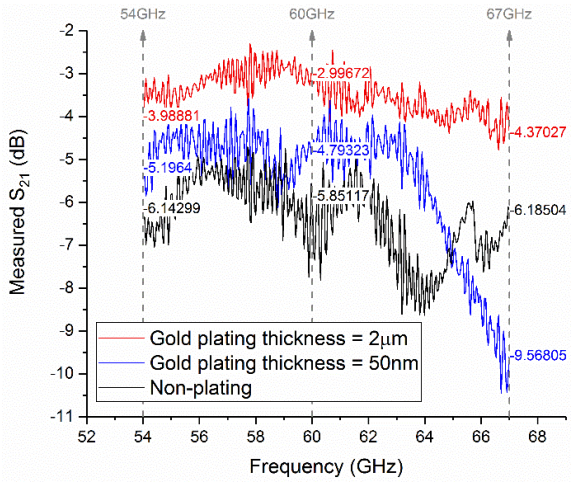

Fig. 6. Measured S_{21} of phase shifters with diverse gold-plating thicknesses.

The increase of the plating to 2µm reliably addresses the elevated metal loss problem caused by oxidation and tarnishing, as verified by a wideband improvement in S_{21} across 54-67 GHz, supported by the surface profiles in Fig. 4 (c) and Fig. 5 (c). It is experimentally verified that 2µm suffices to reliably deter Cu oxidation, while degrading S_{21} by only 0.1 dB compared with a bare Cu-based device simulation assuming no oxidation. Beyond this plated thickness, S_{21} exhibits no further improvement but could be worse due to the increased trapezoidal effects [8][9]. The image of our fully assembled phase shifter with the optimum gold plating is shown in Fig. 1 (b). A figure-of-merit of 60˚/dB is reported at 60 GHz, i.e. a significant improvement by 42˚/dB as compared with [10].

IV. Conclusion

This work numerically investigates and experimentally optimises a novel nickel-free gold-plated ECPW LC-based phase shifter at 60 GHz for broadband last-mile applications [5] [11]. By comparative analysis of adaptive meshing inside metals versus surface impedance model without meshing inside, we derive the threshold that conventional surface impedance model is invalid. Implication of this can be expanded for wider range of millimetre-wave components (e.g. filters, antennas, couplers) with plating thicknesses comparable to penetration depths.

References

[1] M. Nestoros, N. Papanicolaou, and A. Polycarpou, "Design of Beam-Steerable Array for 5G Applications Using Tunable Liquid-Crystal Phase Shifters," 2019 13th European Conference on Antennas and Propagation (EuCAP), Krakow, Poland, 2019, pp. 1-4.

[2] J. Li, "Low-loss tunable dielectrics for millimeter-wave phase shifter: from material modelling to device prototyping," IOP Conference Series: Materials Science and Engineering, 2020.

[3] L. Cai, H. Xu, J. Li, and D. Chu, "High figure-of-merit compact phase shifters based on liquid crystal material for 1–10 GHz applications," Jpn. J. Appl. Phys., vol. 56, 011701, November 2017.

[4] L. Cai, H. Xu, J. Li, and D. Chu, "High FoM liquid crystal based microstrip phase shifter for phased array antennas," in 2016 International Symposium on Antennas and Propagation, Okinawa, 2016, pp. 402-403.

[5] J. Li and D. Chu, "Liquid crystal-based enclosed coplanar waveguide phase shifter for 54–66 GHz applications," Crystals, vol. 9, 12, 650, December 2019.

[6] J. Li, H. Xu, and D. Chu, "Design of liquid crystal based coplanar waveguide tunable phase shifter with no floating electrodes for 60–90 GHz applications," in 2016 46th European Microwave Conference (EuMC), London, 2016, pp. 1047-1050.

[7] A. Yontem, J. Li, and D. Chu, "Imaging through a projection screen using bi-stable switchable diffusive photon sieves," Opt. Express, vol. 26, pp. 10162-10170, April 2018.

[8] J. Li, "Managing 60 GHz Field Peaking of an Enclosed Coplanar Waveguide by Core Edge Shaping," International Conference on Numerical Electromagnetic and Multiphysics Modeling and Optimization (IEEE MTT-S NEMO), Hangzhou, 2020.

[9] J. Li, "Structure and Optimisation of Liquid Crystal based Phase Shifter for Millimetre-wave Applications," Apollo, University of Cambridge Repository, doctoral thesis, January 2019.

[10] Y. Garbovskiy, V. Zagorodnii, P. Krivosik, J. Lovejoy, R. Camley, Z. Celinski1, A. Glushchenko, J. Dziaduszek, and R. Dabrowski, "Liquid crystal phase shifters at millimetre wave frequencies," J. Appl. Phys., vol. 111, 054504, March 2012.

[11] J. Li, "Fault-Event Trees Based Probabilistic Safety Analysis of a Boiling Water Nuclear Reactor's Core Meltdown and Minor Damage Frequencies," Safety, vol. 6, 2, 28, June 2020.